Lim et al
SUPPLEMENTARY INFORMATION

I. METHODS

Surface biotinylation & Western blotting. Fractions of the surface protein of INS-1 cells were incubated with using surface biotinylation EZ-Link sulfo-NHS-SS-Biotin (Pierce, USA). The cells were homogenized with RIPA buffer (50 mM Tris-HCl, 150 mM NaCl, 1% Nonidet P-40, 0.25% sodium deoxycholate, 1 mM EDTA) and protease inhibitor (Sigma). The cell lysates were centrifuged at 10,000 *g* for 2 min at 4 ºC to remove debris of cell. The samples were incubated with NeutrAvidin™ Gel slurry for 1hr. Then the bead-bound proteins were eluted with SDS sample buffer containing 10% β-mercaptoethanol and 50 mM DTT for 1hr to get the surface membrane proteins. The proteins were resolved by 12% SDS-PAGE and blotted onto PVDF membranes. The surface and total expression levels of Kir6.2 were determined by western blot analysis using antibody of Kir6.2 (1:1000, Santa Cruz Biotechnology, USA). To confirm the consistent amount of the surface proteins, the membrane detected by Kir6.2 primary antibody was washed by using the washing buffer (0.1% SDS, 1% Nonidet P-40 in PBS) for 2hrs and then blocked with 4% skim milk in PBS containing 0.2% Tween-20. The membrane was incubated overnight with Kir2.1 primary antibody (1:1000, Santa Cruz Biotechnology, USA) at 4 ºC and then with secondary goat anti-rabbit (1:2000, Abcam, UK) at RT for 1 hr. Protein was visualized using the ECL advance western blotting detection kit (Amersham Biosciences, UK). The total expression level of AMPK was probed with Western blot analysis using the antibody to AMPKα (Cell Signaling, USA). To examine AMPK activation directly in our experimental conditions, the level of phosphorylated-AMPK was measured using phospho-AMPKα (Thr172) antibody (Cell Signaling, USA). The relative band intensities were compared via band scanning using a Gel Doc® XR (Bio-Rad, USA) with Quantity One software, version 4.5.2.

AMPK siRNA. Small interfering RNAs were synthesized by Dharmacon Research. The 19-nucleotide (plus 2 nucleotides at the 5' end) siRNA sequences were as follows: α1-AMPK, GCAUAUGCUGCAGGUAGAU (nucleotides 738–756, Acc. No. NM019142); α2-AMPK, CGUCAUUGAUGAUGAGGCU (nucleotides 865–883, Acc. No. NM023991), and scrambled siRNA, AUUGUAUGCGAUCGCAGAC. INS-1 cells in 60-mm dishes at 80% confluence were transfected with both α1- and α2-AMPK siRNA (2 μg each), or scrambled siRNA (4 μg) according to the manufacturer's instructions using Nucleofector (Amaxa). When GFP was co-transfected, the estimated GFP-positive fraction was about 50%. All siRNA experiments were performed 48 h after transfection.

Verification of Kir6.2 antibody. We confirmed that no specific labeling occurred in INS-1 cells stained with the fluorescent-labeled secondary antibodies alone (Fig. S10*A*). Antibody specificity was verified by observing zero immunoreactivity in HEK293 cell lines, which have little (if any) endogenous expression of K_{ATP} channel proteins (Fig. S10*B*).

Measurement of insulin secretion from pancreatic islets. Islets of Langerhans were isolated from the pancreata of male Sprague-Dawley rats, each weighing 200-250 g, by a collagenase digestion technique. Prepared islets were cultured in RPMI-1640 media with 11.1 mM glucose in a humidified atmosphere of 5% CO_2 in air at 37°C. For 24 hr before experiments, those islets were incubated in RPMI media containing 5 mM glucose. Then the media was changed with 3 mM glucose-containing KRB buffer (114 mM NaCl, 4.4 mM KCl, 1 mM $MgSO_4$, 29.5 mM $NaHCO_3$, 1.28 mM $CaCl_2$, 0.1% BSA, 10 mM HEPES, pH adjusted to 7.4) and maintained for 1 hr. Compound C or AICAR was treated from this time. The islets were moved by hand-picking to the buffer containing 11.1 mM glucose where the sampling for insulin measurement started. After 1 hr, the buffer was changed with glucose-free KRB buffer. The sampling was taken only one time in each independent 10 size-matched islets containing batch at 30 min after exposure to 11.1 mM glucose, 0 min, 30 min, 60 min, 90 min and 120 min after exposure to 0 mM glucose. Obtained values were normalized to show the amount of secreted insulin during 30 min just before the

indicated times. Insulin secretion from islets was measured by enzyme immunoassay and expressed as μg of proteins. The cell-containing media were centrifuged (700 *g*, 5 min), and the supernatant (200 μl) was carefully collected and stored (-20°C). To determine insulin content, the remaining islet pellet was washed in 400 μl RPMI-1640 medium and lyzed in 150 μl ice-cold lysis buffer (50 mM HEPES, 0.1% Triton X-100, 1 μM PMSF, 10 μM E-64, 10 uM pepstatin A, 10 μM TLCK, 100 μM leupeptin; pH 8.0). After sonication and centrifugation (10,000 *g* for 2 min), the resultant supernatant was assayed for final insulin content expressed as μg of proteins. Total islet insulin content was calculated by adding insulin secreted into the supernatant plus final insulin content. Percentage of islet insulin content secreted was calculated for each data point. Rat insulin ELISA kits were purchased from Mercodia (Uppsala, Sweden). The number of each data point was six obtained in at least three-independent experiments.

II. Interpretation of single channel data

In principle, higher *NPo* can be caused by increasing the number of functional channels (*N*) or by increasing the open probability (*Po*). However, the measurement of G_{max} or *NPo* cannot distinguish these two possibilities. We could not directly measure *N*, but only measure the maximum number of channels opened at the same time (*N'*). In principle, the probability that all *N* channels open simultaneously is Po^N. This means that if there are six channels and *Po*=0.1, the probability that six channels open simultaneously is 10^{-6} (corresponding to 0.06 ms opening during 1 min recording), which is very unlikely to be observed. Accordingly, estimation of *N* from *N'* has always a risk for underestimation and the gap gets larger as *N* increases.

We showed in the present study that *N*' increased by about two folds, while *NPo* increased about 5 folds in GD-treated cells. But, for the reason that explained above, this difference does not mean that the *Po* increases 2.5 fold in GD. In fact, the increase in *NPo* by GD treatment was similar to the increase in surface Kir6.2 levels measured using biotinylation assay, indicating that changes in *NPo* measured from excised patches under the condition that maximize *Po* in the presence of diazoxide are mainly attributable to the changes in *N*.

We found that the chance of having active K_{ATP} channels in the patch membrane was significantly higher in GD-treated cells (21 of 24 trials) compared to 11G-treated cells (16 of 32 trials), and that the maximum number of channels opened at the same time (*N'*) was also significantly more in GD-treated cells (Fig. 1*E*).

There was no evidence that ATP-sensitivity or kinetics of channel gating (mean open time) was affected by glucose deprivation (Fig. S1 and S2).

III. Comparison of experimental conditions with previous studies

In Table S1, we summarized the K_{ATP} conductance (G_{max}) and the experimental protocols used in our study, Yang *et al*. (1), and Smith *et al*. (2). In spite of number of differences in experimental protocols and cell types, G_{max} obtained in cells incubated in low glucose (LG; 3 mM or 0 mM) is not greatly different among different studies (from 2.48 to 3.28 nS/pF). However, G_{max} obtained in control (11.1 mM) or high glucose (HG; 17, or 25 mM)-treated cells is strikingly different (0.33 *vs* 3.87 nS/pF). If G_{max} obtained in control or HG-treated cells is compared with that in LG-treated cells in each study, it is ~30% increase in Yang *et al*. (1), ~30% decrease in Smith *et al*. (2), and ~90% decrease in our study in INS-1 cells. Why G_{max} in 11G-treated cells in our study is exceptionally smaller than other studies? Do some factors in our experimental condition inhibit whole-cell K_{ATP} currents in 11G-treated cells or do some factors in other studies increase whole-cell K_{ATP} currents in 11G-treated cells? Currently, there is no clear answer, but we examined if differences in experimental protocols may give a clue to understand the discrepancy.

A number of differences (cell type, duration and temperature of pre-treatment) were noticed, but we focused on differences in the composition of internal solutions (Table S1). K_{ATP} channel currents were activated by application of diazoxide in the presence of ATP and ADP (0.3 mM in Yang *et al*. (1), and 0.1 mM in Smith *et al*. (2)), whereas we used ATP- and Mg^{2+}-free internal solutions. Since whole-cell K_{ATP} currents were recorded by washing-out ATP via patch pipettes, cellular energy states should be converted to low energy state during cell dialysis. According to our experiments, it takes several minutes. Various cellular events may occur during this time, and these changes can be greatly affected by internal solutions. We wondered whether energy-dependent signaling, such as AMPK activation, can be activated during cell dialysis with internal solutions containing low MgATP resulting K_{ATP} channel recruitment.

To examine this possibility directly, we measured K_{ATP} current density in our cells using 0.3 mM ATP containing internal solutions in the presence of diazoxide (0.25 mM), and tested effects of compound C. G_{max} in GD-treated cells obtained under this condition was 3.62 ± 0.47 nS/pF (n = 9). The effect of changing experimental conditions on K_{ATP} current activation was striking in 11G-treated cells; G_{max} was 2.07 ± 0.22 nS/pF (n = 9). To test whether AMPK activation is involved in K_{ATP} currents recorded under this condition, we tested the effect of compound C. In both GD- and 11G-treated cells, K_{ATP} currents were almost completely inhibited by compound C (Fig. S10). This result is consistent with the idea that AMPK activation is involved in K_{ATP} current activation by acute dialysis of cells with low concentration of MgATP in the presence of diazoxide. It is thus suggested that to measure K_{ATP} conductance that represents the effects of pre-treatment in normal glucose solution, it is required to inhibit activation of low-energy dependent signaling such as AMPK during ATP wash-out. It appears that AMPK is not readily activated during ATP wash-out with Mg^{2+}- and ATP-free internal solutions, as was used in our study, so that G_{max} in 11G-treated cells is low. We speculated that Mg^{2+} may be required for AMPK activation, but this possibility needs to be investigated in future studies.

REFERENCES

1. Yang SN, Wenna ND, Yu J, Yang G, Qiu H, Yu L, Juntti-Berggren L, Kohler M, Berggren PO: Glucose recruits K(ATP) channels via non-insulin-containing dense-core granules. *Cell Metab* 6:217-228, 2007

2. Smith AJ, Partridge CJ, Asipu A, Mair LA, Hunter M, Sivaprasadarao A: Increased ATP-sensitive K+ channel expression during acute glucose deprivation. *Biochem Biophys Res Commun* 348:1123-1131, 2006

Table S1

	K_{ATP} conductance (nS/pF)		Voltage range for conductance measurement (mV)	Solution (mM)	
	incubated in low glucose	incubated in normal or high glucose		internal	external glucose
Yang *et al*. (mouse pancreatic β-cells)	3.15 (1 hr in 3 mM)	3.87 (1 hr in 17 mM)	-60 ~ -80	0.3 MgATP 0.3 K_2ADP 1 $MgCl_2$	Same as in incubation solution
Smith *et al*. (INS-1 cells)	3.28 (overnight in 3 mM)	2.14 (overnight in 25 mM)	+100 ~ -100	0.1 MgATP 0.1 ADP 0.6 $MgCl_2$	Same as in incubation solution
Present study (INS-1 cells)	2.48 and 2.28 (2hr in 0 and 3 mM at RT)	0.33 (2 hr at 11.1 mM at RT)	-70 ~ -130	0 ATP, 0 Mg^{2+}, 5 EDTA	0 mM

Figure S1. Analysis of single channel kinetics in 11G- and GD-treated INS-1 cells
(A) Representative open time histogram analyzed from single K_{ATP} channel current–recorded at 0 mV from a cell-attached patch in 11G- (left panel) and GD- (right panel) treated INS-1 cells. Mean open time was obtained by fitting the histogram with a single exponential function. **(B)**. The summary bar graph for mean open time showed no significant difference between 11G- and GD- treated cells (1.65 ± 0.12 *vs* 1.72 ± 0.21). Statistical significance was evaluated by unpaired t-test.

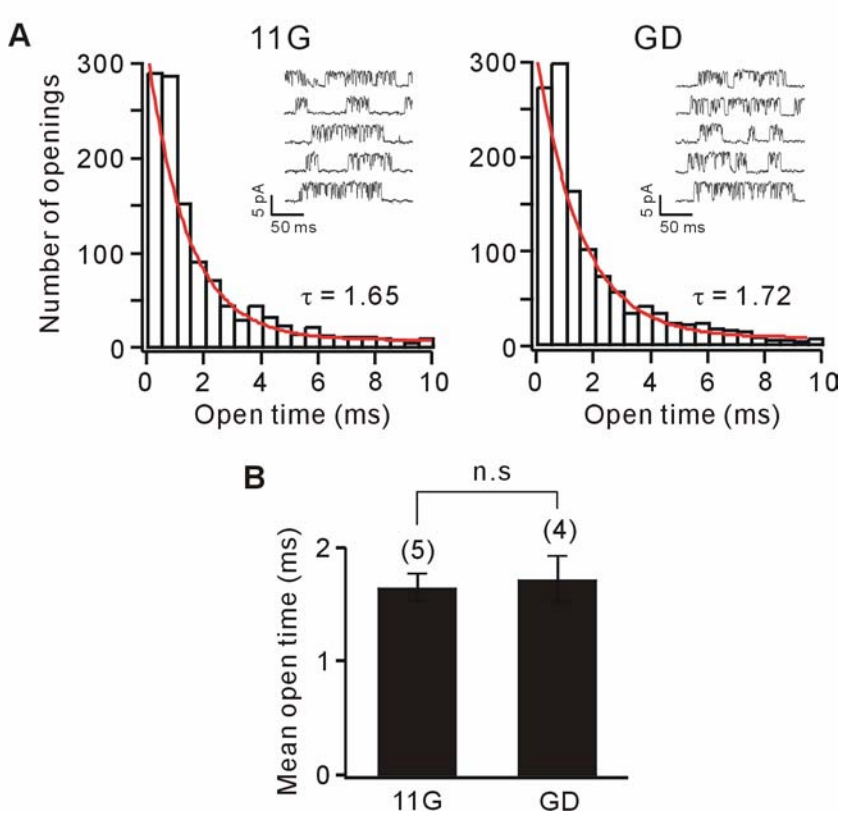

Figure S2. ATP concentration-inhibition relationships in 11G- and GD-treated INS-1 cells
From *NPo* data shown in Fig. 1E, ATP concentration-inhibition curves were obtained. *NPo* values obtained at varying [ATP] were normalized to the value obtained at [ATP] = 0.001 mM, and fitted with the following equation; $y = 1/[1+([ATP]/IC_{50})^h)$, where IC_{50} is the ATP concentration producing half-maximal block and *h* is the Hill coefficient. The solid lines indicate the best fit of the above equation to the mean data obtained from 11G-treated cells (IC_{50} = 4.7 μM, *h* = 1.92, left panel), and GD-treated INS-1 cells (IC_{50} = 4.2 μM, *h* = 1.99, right panel).

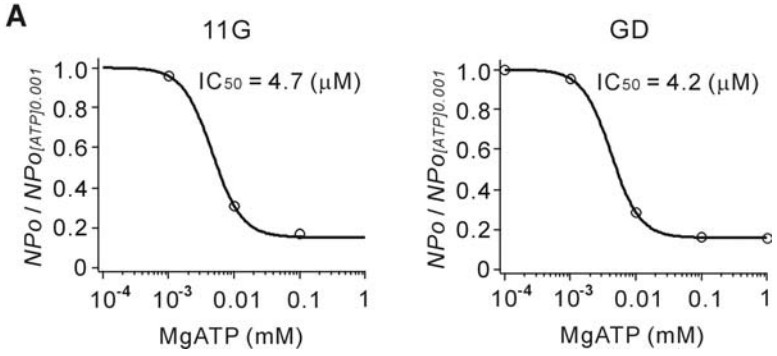

Figure S3. Effects of compound C on K_{ATP} currents in various experimental conditions

(A) Representative whole-cell current trace recorded from GD-treated INS-1 cells by adding 10 μM compound C to internal solution. Whole-cell currents were generated by ± 20 mV voltage pulses (500 ms), from a holding potential of –70 mV every 10s. **(B)** Single-channel K_{ATP} currents recorded at –60 mV in the inside-out patch excised from GD-treated INS-1 cells in the presence of 0.25 mM diazoxide and 0.01 mM MgATP in the bath solution. Application of 10 μM compound C (CC) to the intracellular side (indicated as horizontal bar over current trace) did not affect K_{ATP} channel activity. Channel activities recorded before (a), in the presence (b), and after (c) CC are shown in an expanded time scale in the lower panel. Dotted line: closed level.

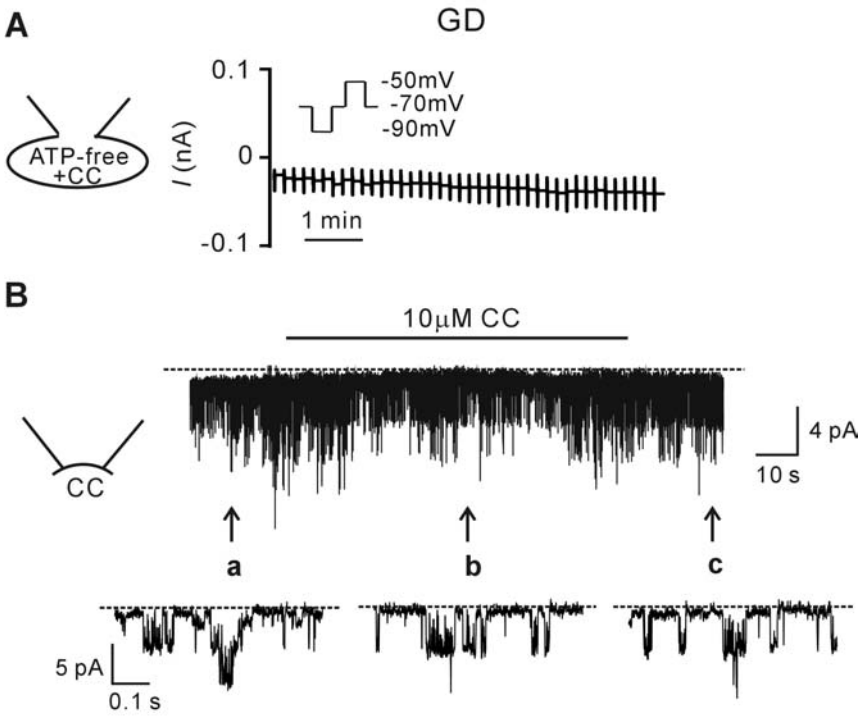

Figure S4. AMPK is involved in glucose deprivation-induced increases in K_{ATP} conductance in pancreatic β-cells

(A) Representative recordings of K_{ATP} whole-cell currents obtained in 11G- and GD-treated pancreatic β-cells. Experimental protocols were same as what was used for INS-1 cells in Fig1. **(B)** The summary graph displays normalized average G_{max} (in nS/pF); 1.55 ± 0.23 (n = 11) in 11G, 3.06 ± 0.31 (n = 11) in GD, 0.48 ± 0.09 (n = 4) in GD+CC and 3.67 ± 0.55 (n = 7) in 11G+AICAR. Statistical significance was evaluated by one-way ANOVA. ** $p < 0.01$, *** $p < 0.001$.

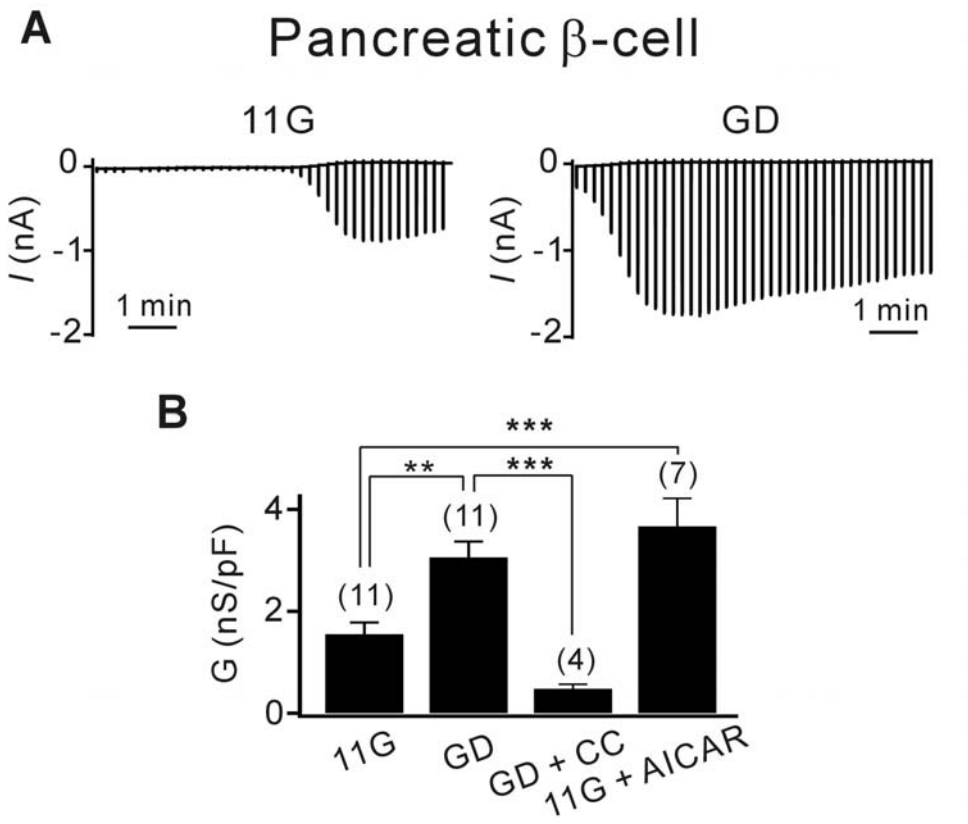

Figure S5. Test for AMPK knockdown using AMPKα siRNA in INS-1 cells and the influence of various factors on Kir6.2 surface expression and AMPK activation.

(A) The total expression levels of the α-subunit of AMPK in the cells transfected with AMPKα siRNA (siAMPK) were significantly reduced compared with those in the cells transfected with an equal concentration of scrambled siRNA (Scr). Similar results were observed in three more trials. Glucose concentration did not affect the total AMPK levels. **(B)** Treatment with 0.25 mM diazoxide containing 11G for 2 h failed to mimic the effect of glucose deprivation on the surface expression level of Kir6.2 and the total level of pAMPK in INS-1 cells (column 1). The surface expression level of Kir6.2 and the total level of pAMPK in 11G-, 6G-, and GD-treated INS-1 cells (column 2,3, and 4). Those in 6G-treated cells were slightly larger compared with 11G-treated cells but much smaller compared with GD-treated cells. Treatment of 40 μM CC only for short time (5 min) in GD remarkably decreased the surface expression level of Kir6.2 and the total level of pAMPK (column 5). The total level of Kir6.2, the surface level of Kir2.1, the total level of AMPK, and the total level of actin was not affected by various factors.

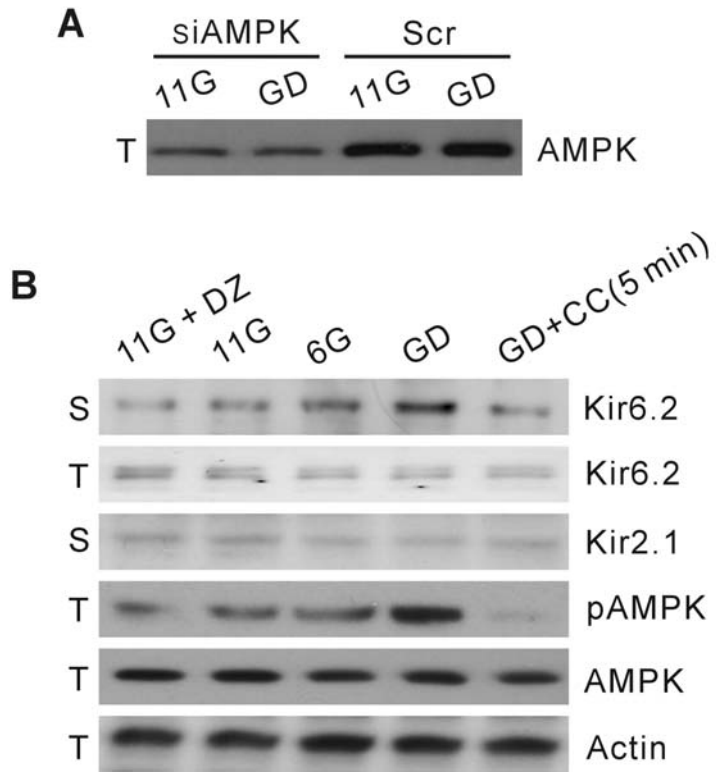

Figure S6. Subcellular distribution of Kir2.1 as a positive control of a surface expressed protein in pancreatic β-cells.

(A-B) Subcellular distribution of Kir2.1 observed in 11G- **(A)** and GD- **(B)** treated pancreatic β-cells showed no significant difference. Nucleus was stained with DAPI (*blue*, first panel) and plasma membrane was stained with DiI (*red*, third panel). Overlay of the fluorescence images showing Kir2.1, DAPI, and DiI (fourth panel). Scale bar: 2 μm.

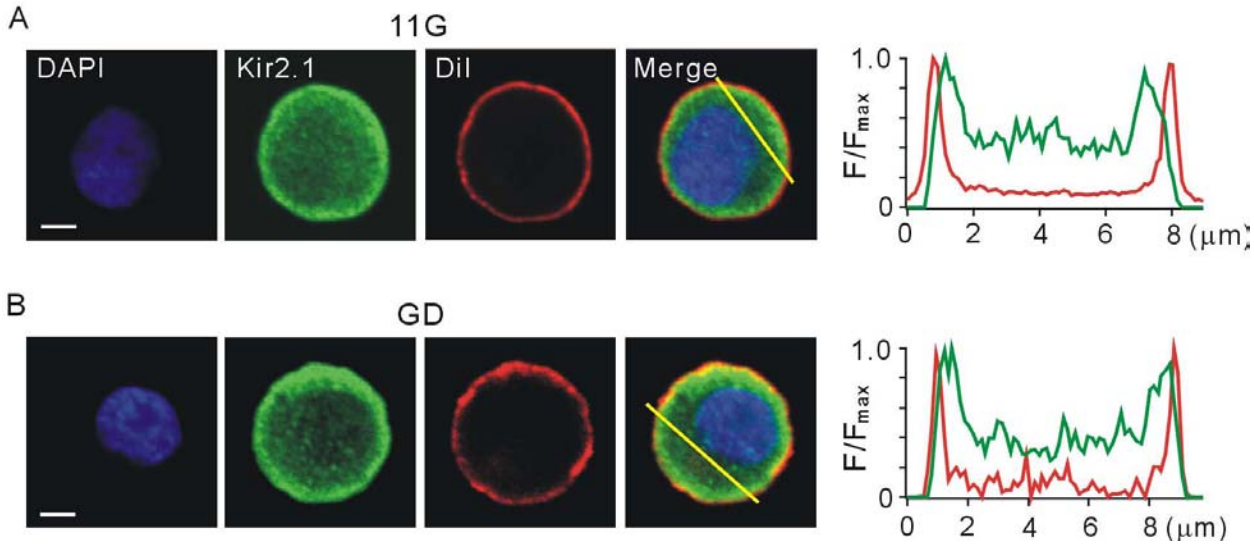

Figure S7. AMPK increases colocalization of Kir6.2 and SUR1 subunits at the cell periphery. **(A)** Confocal fluorescent images obtained from pancreatic β-cells immunolabeled with Kir6.2 (green) and SUR1 (red) antibodies (upper panel). Scale bar: 10 μm. 11G, GD, and GD+CC represent pretreatment conditions as detailed in Fig. 1. Lines of 10 μm length (yellow) were drawn across the cell membrane, taking care to avoid the nucleus, to obtain fluorescence intensity line profiles (lower). **(B)** Mean distribution profiles of Kir6.2 fluorescence intensity. Line profiles obtained from 10-12 cells in each group were averaged, and positions where fluorescence intensity began to rise were assigned as d = 0 to calculate the mean value. The distribution patterns of SUR1 were similar to those of Kir6.2. **(C)** Surface localization indicated as the fluorescence intensity ratio of surface to cytosol. Fluorescence intensities on cell surfaces (s) and in the cytosol (c) were calculated by averaging normalized intensity values between d = 0.6 and 1.2 μm (indicated as "s" in **(B)**) and between d = 3.2 and 3.8 μm (indicated as "c" in **(B)**), respectively. Statistical significance was evaluated by unpaired *t*-test. ** $P < 0.01$. **(D)** Effects of AICAR on the distribution of Kir6.2 (green) and SUR1 (red) immunofluorescence. Note their preferential localizations to the plasma membrane. **(E)** The surface to cytosol ratios of the mean normalized intensities of Kir6.2 and SUR1 signals in AICAR-treated cells (lower, solid bars) were similar to those in GD cells (lower, open bars).

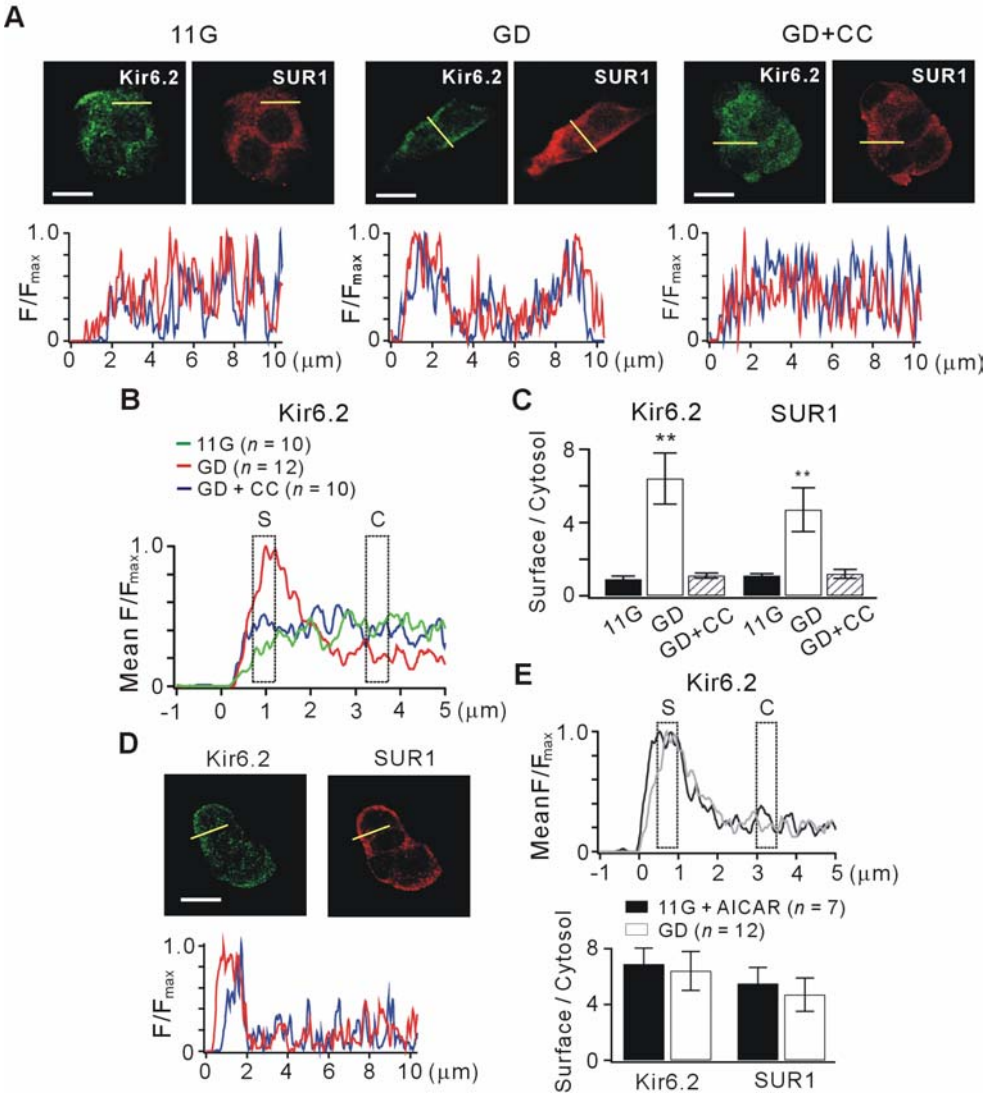

Figure S8. Two-step model for glucose-dependent activation of K_{ATP} channels

In response to glucose deprivation in pancreatic β-cells, AMPK activation is expected to occur in the earlier stage. AMPK-dependent signaling regulates K_{ATP} channel trafficking and contributes to the regulation of number of available channels at the surface membrane. Further decrease in ATP level leads to the opening of K_{ATP} channels, which results in hyperpolarization of β-cell membrane potentials.

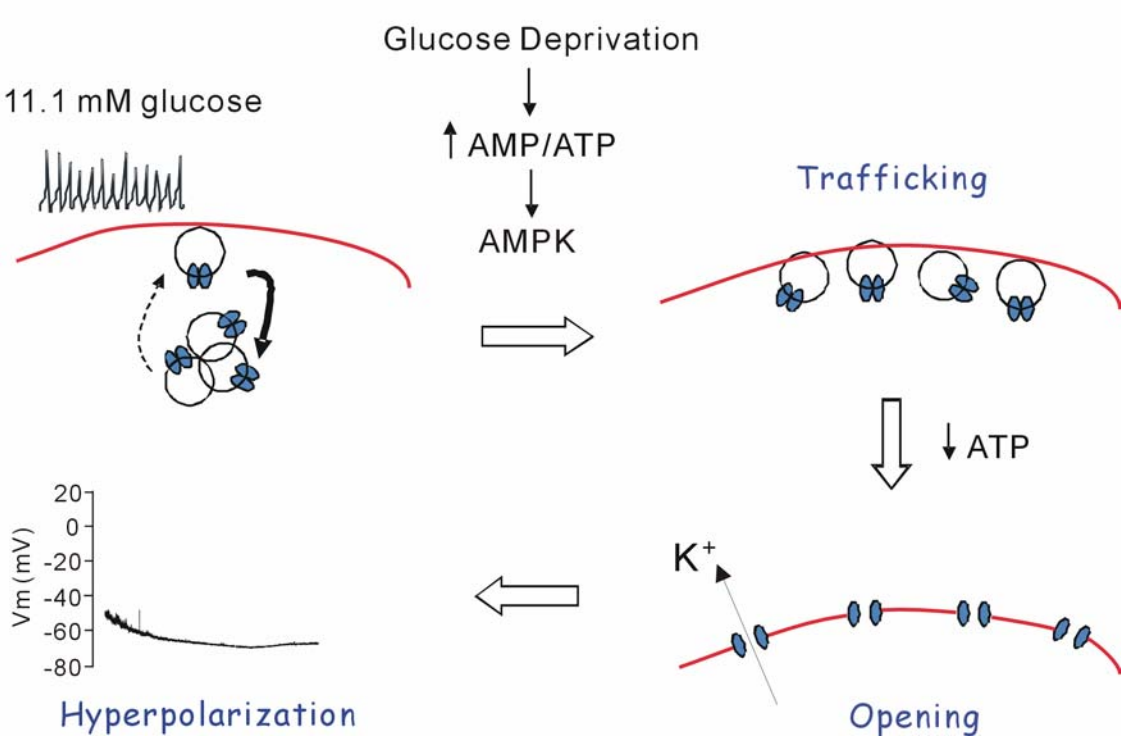

Figure S9. Tests for specificity of antibodies used in the present study

(A) No specific labeling was observed in INS-1 cells stained with the fluorescent-labeled secondary antibodies alone. **(B)** When HEK293 cells, which has little if any endogenous expression of K_{ATP} channel, were treated with anti-Kir6.2 and the fluorescent-labeled secondary antibodies with the same protocol used for INS-1 cells, immunoreactivity was not observed, indicating that non-specific binding was negligible. Scale bar: 20 μm.

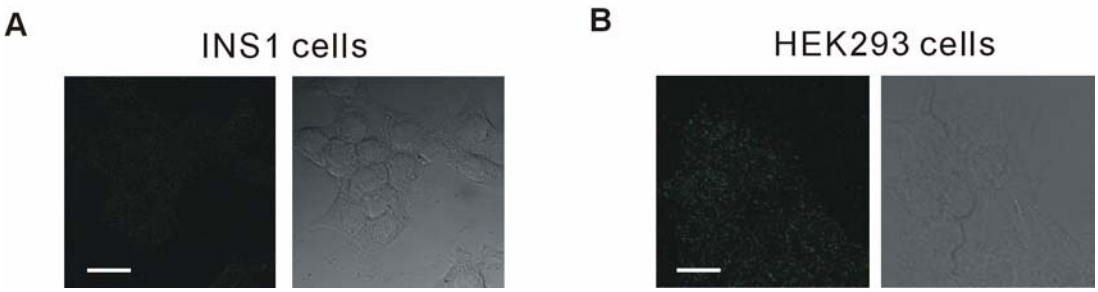

Figure S10. Effects of compound C on whole-cell K_{ATP} currents recorded in the presence of 0.3 mM MgATP and diazoxide.

(A) Whole-cell currents were recorded from 11G or GD-treated INS-1 cells dialyzed with 0.3 mM MgATP and exposed to 0.25 mM diazoxide (DZ), where ± 20 mV voltage pulses (500 ms) were applied from a holding potential of –70 mV every 10s. 10 μM compound C was applied when increases of K_{ATP} currents reached steady state. **(B)** The summary graph displays normalized average G_{max} (in nS/pF) ; 2.03 ± 0.30 in 11G before CC treatment *vs* 0.22 ± 0.08 in 11G after CC treatment (n = 6) and 3.35 ± 0.64 in GD before CC treatment *vs* 0.25 ± 0.05 in GD after CC treatment (n = 6). CC: compound C. Statistical significance was evaluated by unpaired t-test. *** $p < 0.001$.